

Pilot scale study of Co-Fe-Ni nanocatalyst for CO hydrogenation in Fischer-Tropsch synthesis

Hamid Reza Azizi^{a,*}, Ali Akbar Mirzaei^b, Razieh Sarani^b, Massoud Kaykhai^b

^aYoung Researchers Club, South Tehran Branch, Islamic Azad University, Tehran, Iran.

^bDepartment of Chemistry, University of Sistan and Baluchestan, Zahedan, Iran.

Received 24 June 2018; received in revised form 29 December 2018; accepted 27 February 2019

ABSTRACT

In this work, a Co-Fe-Ni catalyst was prepared and the effect of a range of operational variables such as gas hourly space velocity (GHSV), calcination temperature, calcination time and agent on its catalytic performance for green-fuels production was investigated. By application of different characterization techniques such as XRD, BET, TGA/DSC, and SEM, it was found that these parameters have great effects on the structure, porosity, morphology and physic-chemical properties of this catalyst. The optimum conditions were found for the samples which were calcined at 550 °C in air for 6 hours, and operated at 300 °C and 4800 h⁻¹ as the reaction temperature and GHSV respectively. Results also revealed that any increase in the calcination temperature promotes the product shifting towards heavier hydrocarbons (more C₅₊ production). Calcination in air atmosphere was more effective than calcination in N₂ atmosphere.

Keywords: Co-Fe-Ni catalyst, Fischer-Tropsch synthesis, Calcination, Heavy hydrocarbons, Co-precipitation.

1. Introduction

Fischer-Tropsch synthesis (FTS) is a catalytic process which converts the syngas produced from coal, natural gas and biomass resources into liquid fuels or chemicals and assumes to be an important route for the production of green petroleum-based products in the near future [1-5]. The superior feature of liquid hydrocarbons in produced fuel caused that FTS reaction has gain more interest to be applied in chemical plants [6]. It is well known that the research and development of catalysts play an important role in all processes of catalytic reactions and consequently in the FTS reaction [6-8]. Despite the large number of papers published about catalytic effects of transition metals at group VIII, especially cobalt, iron, nickel and ruthenium, only the first two are used for large-scale production in FTS due to their suitable cost and availability [9,10]. Cobalt-based catalysts research is mainly focused on the improvement of its activity and selectivity toward the production of long chain paraffins with the narrow product distribution and resistance to catalyst deactivation [11].

Many studies have argued that using bimetallic catalysts obtained from metal alloys may have some special advantages in FTS, thus mixed oxide catalysts are very important for the conversion of synthesis gas to desired products in industrial uses. However, many multi-metallic systems create synergistic effects which produce highly active, selective and stable catalysts due to variations in both their electronic and geometric structures. In such cases, the catalytic performance is being determined by the atomic composition of the crystallite surface and not merely by the overall bulk composition [12]. Modification of the traditional Fischer-Tropsch catalysts (Fe, Co) by promoters and supporters has provided a means for manipulating the FT products range [13-17]. Ni-based catalysts did not commercialize in FTS because they generally produce lighter products shifted towards methanation and volatile carbonyls at commercial FTS temperatures [18,19]. Despite these issues, nickel has been attracted increasing interest as one of the promoters of catalysts because it can act as a structural promoter to improve the dispersion of active iron and cobalt and can stabilize the catalyst in FT process [20,21]. Moreover, presence of Ni had a positive impact on the catalytic activity and its deactivation rate [22]. Besides, in one of our previous

*Corresponding author.

E-mail address: h.azizi_2011@yahoo.com (H.R. Azizi)

works, we proved that presence of nickel in catalyst can reduce the reduction temperature of FTS [23]. Developing of nickel catalysts in FTS in 30's is briefly summarized by Storch [24] and Pichler [25]. Perhaps the most important work was done by Fischer and Meyer [26] on the application of nickel catalysts in the gasoline synthesis at atmospheric pressure. During the mid-80's, Hadjigeorghiou and Richardson [20,21] did extensive work on co-precipitated NiO/Al₂O₃ catalysts and compared it to Ni supported on a wide range of other supports. While there are many contributions that emphasize on catalyst manufacturing and optimization, kinetic modeling, mechanism and reactor modeling, only a few of them were focused on the effect of operating parameters such as temperature, and feed gas velocity as significant factors which are effective on the selectivity of the products.

This paper aims to investigate the effects of numerous calcination and operating parameters, including temperature, time, agents, and gas hourly space velocity (GHSV) on the product selectivity in FTS. Herein, we report the influence of these parameters on the catalytic performance of Co-Fe-Ni catalyst which was prepared by the co-precipitation method using nitrate multi-hydrate as the precursor salt. Characterization of the catalysts was carried out using XRD, SEM, TGA/DSC and adsorption-desorption measurements such as BET methods.

2. Experimental

2.1. Materials

In this research, Na₂CO₃, Co(NO₃)₂.6H₂O, Fe(NO₃)₃.9H₂O and Ni(NO₃)₂.6H₂O were of reagent grade and were obtained from Merck KGaA, Germany.

2.2. Catalyst preparation

In this study, a cobalt-iron-nickel catalyst with composition ratio of 60:30:10 wt% was prepared using the co-precipitation method as follows: Aqueous solutions of Co(NO₃)₂.6H₂O (2M), Fe(NO₃)₃.9H₂O (2 M) and Ni(NO₃)₂.6H₂O (2 M) were prepared and premixed together. The resulting solution was heated to 70 °C in a round bottomed flask fitted with a condenser. Na₂CO₃ (2 M) solution was added drop-wise to this mixed solution with continuous stirring while the temperature was maintained at 70 °C until pH = 9.3 was achieved. The resulting precipitate was left in this condition for 1 h. The aged suspension was filtered and washed several times with warm distilled water. The precipitate was then dried in an oven at 120 °C for 16 h to give a material denoted as the catalyst precursor.

2.3. Catalysts characterization

2.3.1. X-Ray diffraction

Powder X-Ray diffraction (XRD) measurements were performed using a D5000 Siemens (Germany) instrument. Scans were taken with a 2θ step size of 0.02 and a counting time of 1 s using a Cu K_α radiation source generated at 35 kV and 25 mA. Specimens for XRD were prepared by compaction into a glass-backed aluminum sample holder. Data were collected over 2θ range from 5° to 100°.

2.3.2. Scanning electron microscopy

The morphology of the catalysts was observed by means of a Cambridge S-360 scanning electron microscope (SEM) instrument (UK) operating at 20 kV. To avoid charging problems, before starting measurements, samples were coated with gold/palladium for 80 s in 20 s intervals.

2.3.3. BET measurements

BET surface areas, pore volumes and average pore sizes of the catalysts were measured by N₂ physisorption using Quanta Chrome Nova 2000 automated system (USA). Each catalyst sample was degassed under nitrogen atmosphere at 300 °C for 3 h. In order to obtain the BET surface areas, pore volumes and average pore sizes of different samples were evacuated at -196 °C for 66 min.

2.3.4. Thermal gravimetric analysis (TGA) and differential scanning calorimetry (DSC)

The weight changes in the catalyst precursor were measured using the TGA/DSC simultaneous thermal analyzer (model 1500p, Rheometric Scientific, USA) under a flow of dry air. The temperature was raised from room temperature to 700 °C using a linear program heating rate of 10 °C per min. The sample weight was between 15 and 20 mg.

2.4. Catalyst testing

The experiments were carried out in a fixed-bed tubular stainless-steel reactor consisting of a single stainless-steel tube with an inner diameter of 20 mm and length of 40 mm. More details and scheme of this system and calculating of the product distributions were presented in our previous work [23].

In each test, 1.0 g of the catalyst was diluted with quartz wool (1:4 v/v), then loaded and held in the middle of the reactor. The catalyst was pre-reduced in situ atmospheric pressure in a flowing stream of H₂-N₂ (N₂/H₂ ratio=1; flow rate of each gas=30 mL.min⁻¹) at 300 °C for 4 h before exposure to synthesis gas. The

reactor operated about 12 h to ensure steady state operations were reached. The FTS was carried out under the same reaction conditions of $T=300\text{ }^{\circ}\text{C}$, $P=1\text{ bar}$, $\text{H}_2:\text{CO}=1:1$, $\text{N}_2=20\%$ and $\text{GHSV}=4800\text{ h}^{-1}$.

Reactant and product streams were analyzed online using a gas chromatograph (Thermo ONIX UNICAM PRO+ GC, USA) equipped with a $100\text{ }\mu\text{L}$ sample loop, two thermal conductivity detectors (TCD) and one flame ionization detector (FID).

3. Results and Discussion

3.1. Calcination agent

The atmosphere or agent used for calcination of catalyst precursors has a significant influence on the performance of the final catalyst; for example, according to the work of Reinalda and Kars, [27] if during the calcination, the catalyst is exposed to an atmosphere containing large amounts of nitrogen oxides, the activity and selectivity may be enhanced to long chain hydrocarbons. In contrast, van de Loosdrecht et al. [28] recorded high cobalt metal surface areas and high catalytic activities when the nitrogen oxides and water concentrations were kept in low amounts.

In this section, two samples of the catalyst precursor were separately calcined in air and nitrogen agents ($550\text{ }^{\circ}\text{C}$, 6 h at heating rate of $10\text{ }^{\circ}\text{C}\cdot\text{min}^{-1}$). The effect

of calcination atmosphere on catalytic performance in the fixed-bed reactor, percent of CO conversion and product selectivity are shown in Fig. 1.

As can be seen, the catalyst calcined in air at $550\text{ }^{\circ}\text{C}$ for 6 h with a heating rate of $10\text{ }^{\circ}\text{C}\text{ min}^{-1}$ had the highest CO conversion and the highest selectivity ($T=300\text{ }^{\circ}\text{C}$, $\text{H}_2:\text{CO}=1:1$, $P=1\text{ bar}$ and $\text{GHSV}=4800\text{ h}^{-1}$). By taking these results into account, it can be considered that the air is a better calcination agent for this catalyst [29,30]. Characterization of the precursor, fresh (sample which calcined, not tested in FTS) and used catalysts calcined in air and N_2 (before and after the test) was carried out using BET instrument; the specific surface areas (SSA), pore volumes (PV) and pore sizes (PS) of these samples are presented in Table 1.

It was found that the freshly calcined catalyst has a higher specific surface area than the precursor and calcined catalysts (after the test). It is apparent that with calcination of precursor, the BET surface area increases significantly, the average pore diameters decrease slowly, and the pore distributions shift to the small size. This may be due to crystallite growth phenomena or can be attributed to the partial collapse porous iron, cobalt or nickel oxide/hydroxide frame work [29,31]. In addition, decreasing the surface areas of the used catalysts may be due to the formation of carbonaceous species [32] or sintering phenomena after the reaction [29].

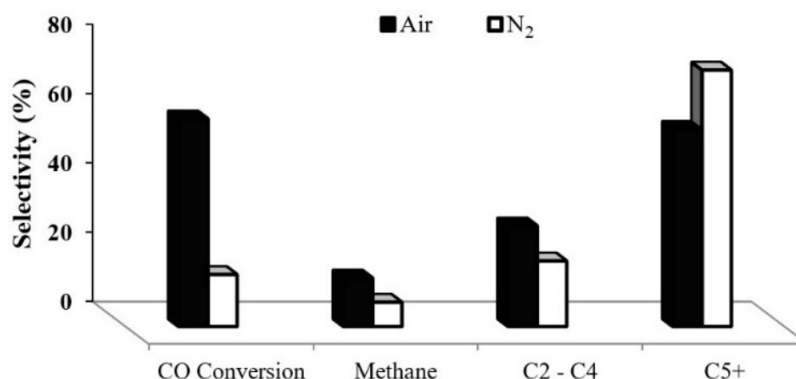


Fig. 1. Effects of calcination agents on the catalytic performance of Co-Fe-Ni catalyst.

Table 1. BET measurements (effect of various agents on the texture).

Samples	SSA ($\text{m}^2\cdot\text{g}^{-1}$)	PV ($\text{cm}^3\cdot\text{g}^{-1}$)	PS (nm)
Precursor	97.3	4.31×10^{-2}	144.20
Fresh calcined at air	157.67	2.28×10^{-2}	116.50
used calcined at air	99.98	3.50×10^{-3}	165.20
Fresh calcined at N ₂	82.94	3.50×10^{-4}	262.4
used calcined at N ₂	78.94	4.15×10^{-4}	269.0

3.2. Calcination temperature

Calcination is generally used to thermally decompose non-oxidic precursors and oxidize the support and surface species. After precursors oxidation, calcination provides thermal energy to active wetting and spreading as the Tammann temperature of the surface oxide is approached [33]. With regard to understanding the calcination temperature influence on the catalytic performance of the catalyst under study, a series of calcination was performed on this catalyst at a temperature range of 400-700 °C for 6 h. All catalysts were tested toward FTS under the same reaction conditions ($T=300$ °C, $P=1$ atm, $H_2/CO=1$ and $GHSV=4800$ h^{-1}). The results obtained were presented in Fig. 2. It is found that by increasing the temperature from 400 °C to 550 °C, CO conversion (activity) increases from about 30% to 60%; also in this

range of temperature, and the temperature rises, C_2-C_4 and C_{5+} selectivity increases; however, CH_4 selectivity decreases. More increments in the temperature (up to 700 °C) cause the CO conversion decreases from 60% to about 45% with an increase in methanation. These results can be due to the coking of catalyst and the increase of the crystallite size of iron or cobalt phases [31, 34]. The sample calcined at 550 °C showed the best catalytic performance (higher activity and lower CH_4 formation) for Fischer-Tropsch synthesis.

In order to investigate phase transforming during the calcination, pretreatment and FTS reaction, all samples (including precursor, calcined samples at different temperatures and tested samples) were analyzed using the X-ray diffraction. The obtained patterns are displayed in Fig. 3.

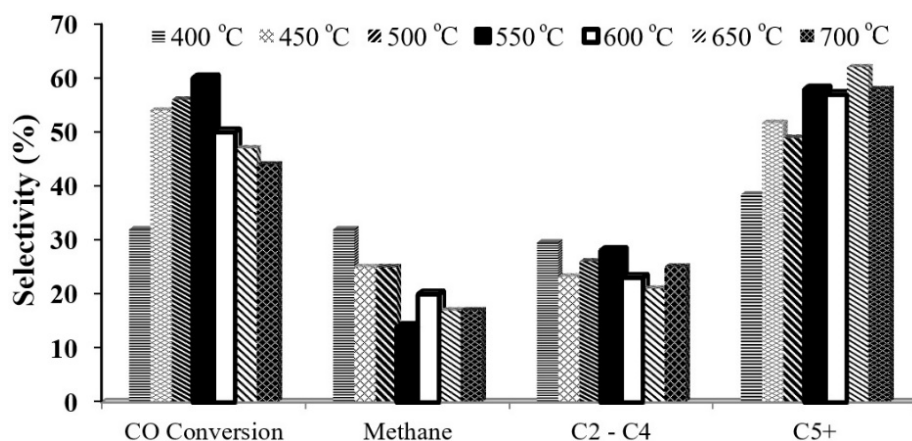


Fig. 2. Effect of calcination temperature on the catalytic performance of Co-Fe-Ni catalyst.

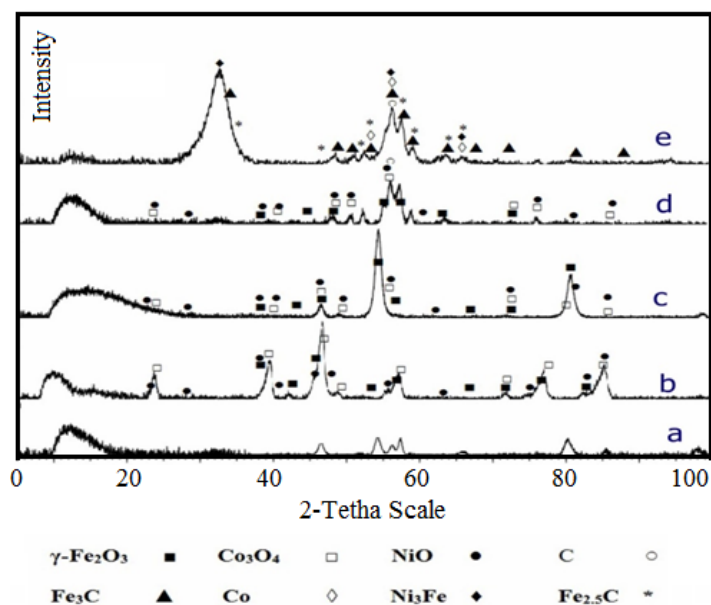


Fig. 3. XRD patterns of precursor and calcined catalysts (a) precursor, (b) calcined at 400 °C, (c) calcined at 550 °C, (d) calcined at 700 °C and (e) the catalyst after the test (calcined at 550 °C).

When the precursor is amorphous or its phases are poorly crystallized or have small crystallite size, due to the broader peaks, no phases could be identified.

As shown in Fig. 3, cobalt oxide, nickel oxide and iron carbide phases are formed by calcination under air condition. As the reduction of the catalyst proceeded, iron oxide was transformed from $\text{Fe}_2\text{O}_3 \rightarrow \text{Fe}_3\text{O}_4 \rightarrow \alpha\text{-Fe}$ or iron carbide. $\alpha\text{-Fe}$ could not be observed in our calcinated catalyst because metallic iron is fairly reactive to the carbons dissociated from carbon monoxide. Also, among the iron carbides, carbides with carbon atoms in octahedral interstices, $\epsilon\text{-Fe}_2\text{C}$ and $\epsilon\text{-Fe}_{2.2}\text{C}$, carbides with carbon atoms in trigonal prismatic

interstices, $\chi\text{-Fe}_{2.5}\text{C}$ and $\theta\text{-Fe}_3\text{C}$, according to the JCPDS card, only $\chi\text{-Fe}_{2.5}\text{C}$ and $\theta\text{-Fe}_3\text{C}$ show a main diffraction peak. Previous results suggested that the most catalytic active phase in FTS is $\epsilon\text{-carbide}$ ($\text{Fe}_{2.2}\text{C}$), which over long periods of reaction is converted into the Haggy carbide ($\chi\text{-Fe}_{2.5}\text{C}$) and subsequently converts into the cementite ($\theta\text{-Fe}_3\text{C}$) with lower carbon content [35,36].

To investigate the influence of calcination temperatures and FTS reaction on the morphology of the catalyst, characterization of catalysts precursor (calcined at 400, 550 and 700 °C) and used (calcined at 550 °C for 6 h) catalysts were carried out using the scanning electron microscopy (SEM) technique (Fig. 4).

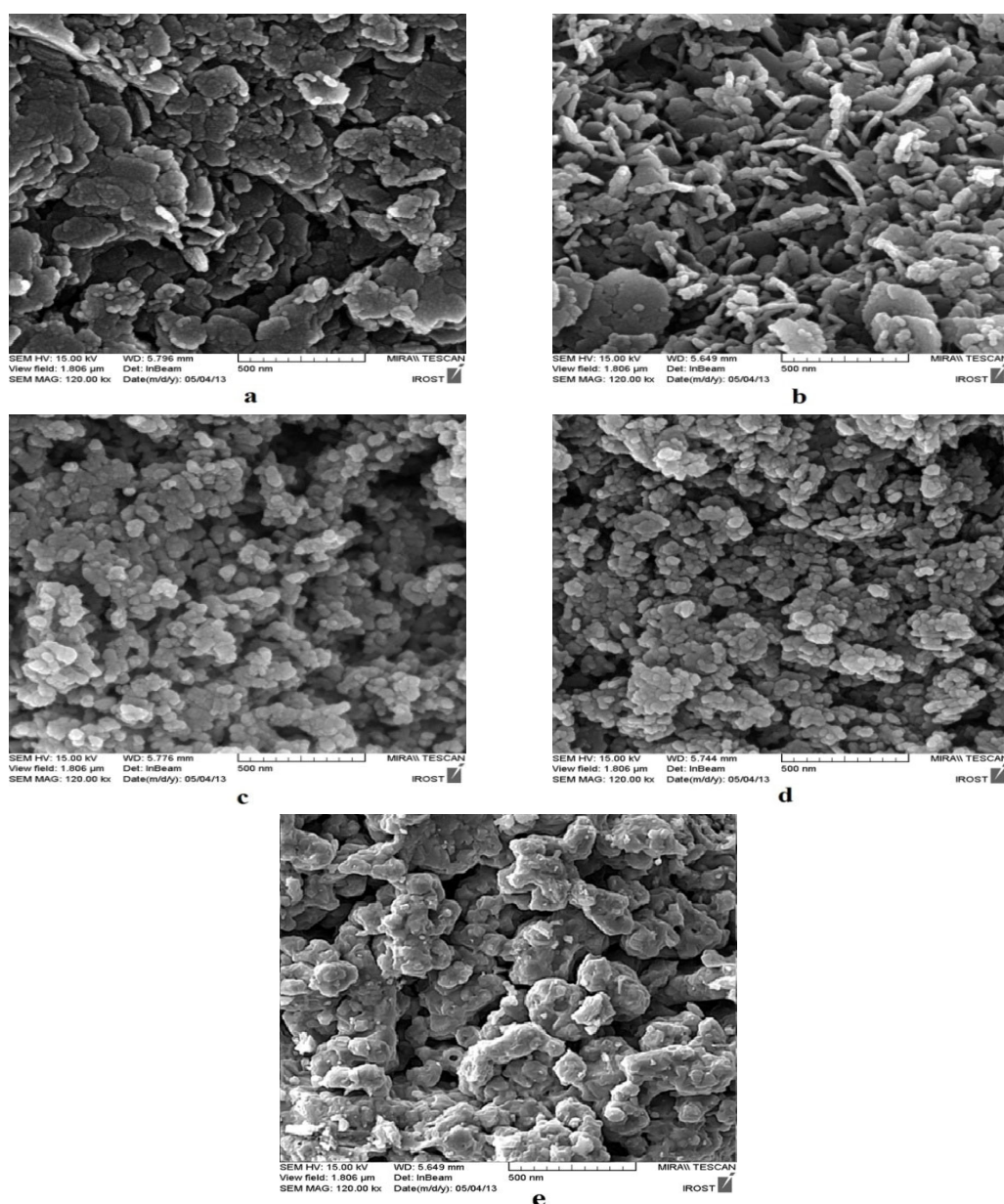


Fig. 4. SEM images of catalysts in (a) precursor, (b) calcined at 400 °C, (c) calcined at 550 °C, (d) calcined at 700 °C and (e) catalyst after the test (calcined at 550 °C).

The SEM images showed differences in morphology of precursor and calcined catalysts. The electron micrograph shown in Fig. 4a it is obtained for catalyst precursor and depicts several aggregations of irregularly shaped particles with different sizes and shapes. After the calcination, the morphological features are different with the precursor sample and shows that the agglomerate size is greatly reduced in comparison with the precursor (Figs. 4b-d). Comparing images 4b, 4c and 4d reveals that by increasing the calcination temperature, the agglomeration and particle size of the catalyst increase. As can be seen, the morphological characteristics of the tested catalyst is absolutely different and uneven, and disproportion agglomerate and size of the tested grains become larger by agglomeration (Fig. 4e); this phenomena may be attributed to sintering phenomena [37].

By using the BJH method, the BET surface, pore volume and average pore size of the catalysts with different calcination temperatures and the nitrogen adsorption-desorption isotherms and pore size distribution curves were calculated and data are presented in Table 2 and Fig. 5. All isotherms are belonging to type IV and exhibit a hysteresis loop which is typical for capillary condensation in the mesoporous. The gradual rise in the range of $0 < P/P_0 < 0.8$ corresponds to filling of micropores with N_2 gas and the sharply short inflection in the range of $0.7 < P/P_0 < 1.0$ indicates the capillary condensation of N_2 in mesopores status. These facts indicate the catalysts are of micro-mesoporous type material.

From the data in Table 2, it is apparent when the calcination temperature goes up to 550 °C (with a constant heating rate), the surface area of the catalyst increases but both pore volume and pore size decrease. By increasing the temperature beyond 550 °C, the reverse trend was found for these three parameters. It is reasonable to assume that the calcinations at the highest temperature causes the sintering of particles in these

precursors or leads to collapse of the porous framework and carbonaceous deposits [38]. From Table 2, it can be observed that the surface area of the catalysts after pretreatment by syngas and after its testing by FTS (used samples) has been decreased, this can be attributed to the agglomeration of catalyst particles during the pretreatment [38].

3.3. Calcination time

If the samples are calcined for long times under direct high temperatures, sintering will happen or the crystalline framework will be changed; therefore, in addition to the temperature, the quality of the FTS products depend on the calcination time, heating rate and calcination reagent. In order to study the effect of calcination time on the catalytic performance, a series of Co-Fe-Ni catalysts were calcined at 550 °C at five different calcination times from 4 to 12 h. The obtained results are presented in Fig. 6.

It was observed that by increasing the calcination time, the activity increases; however, the C_2 - C_4 and C_5+ selectivity was decreased. The sample which was calcined at 550 °C for 10 h showed the highest CO conversion, while the methane production and olefin (C_2 - C_4) selectivity of it was lower than the samples which were calcined for 6 h. Therefore, the sample which was calcined at 550 °C for 6 h selected as the optimal catalyst (considering the highest CO conversion and C_2 - C_4 selectivity, and lowest CH_4 production).

3.4. Reaction temperature

The influence of the reaction temperature at GHSV=4800 h^{-1} under the constant atmospheric pressure on the steady state catalytic performance of the cobalt iron nickel oxide catalyst was investigated at the range of 250-360 °C. The CO conversion and product selectivity for this range were calculated and presented at Fig. 7.

Table 2. BET measurements (effect of various calcination temperatures on the textural).

Catalysts	Fresh calcined			Used calcined		
	SSA ($m^2.g^{-1}$)	PV ($cm^3.g^{-1}$)	PS (nm)	SSA ($m^2.g^{-1}$)	PV ($cm^3.g^{-1}$)	PS (nm)
Precursor	97.3	4.31×10^{-2}	144.20	-	-	-
Calcined at 400 °C	149.43	2.70×10^{-2}	119.30	90.23	5.02×10^{-3}	160.20
Calcined at 450 °C	155.59	2.30×10^{-2}	117.40	89.30	5.31×10^{-3}	162.10
Calcined at 500 °C	158.24	2.21×10^{-2}	115.20	97.34	4.20×10^{-3}	168.50
Calcined at 550 °C	157.67	2.28×10^{-2}	116.50	99.98	3.50×10^{-3}	165.20
Calcined at 600 °C	152.67	2.68×10^{-2}	118.30	96.76	3.61×10^{-3}	170.20
Calcined at 650 °C	147.56	3.11×10^{-2}	124.20	90.21	5.11×10^{-3}	175.50
Calcined at 700 °C	140.45	3.20×10^{-2}	123.20	86.32	5.01×10^{-4}	173.80

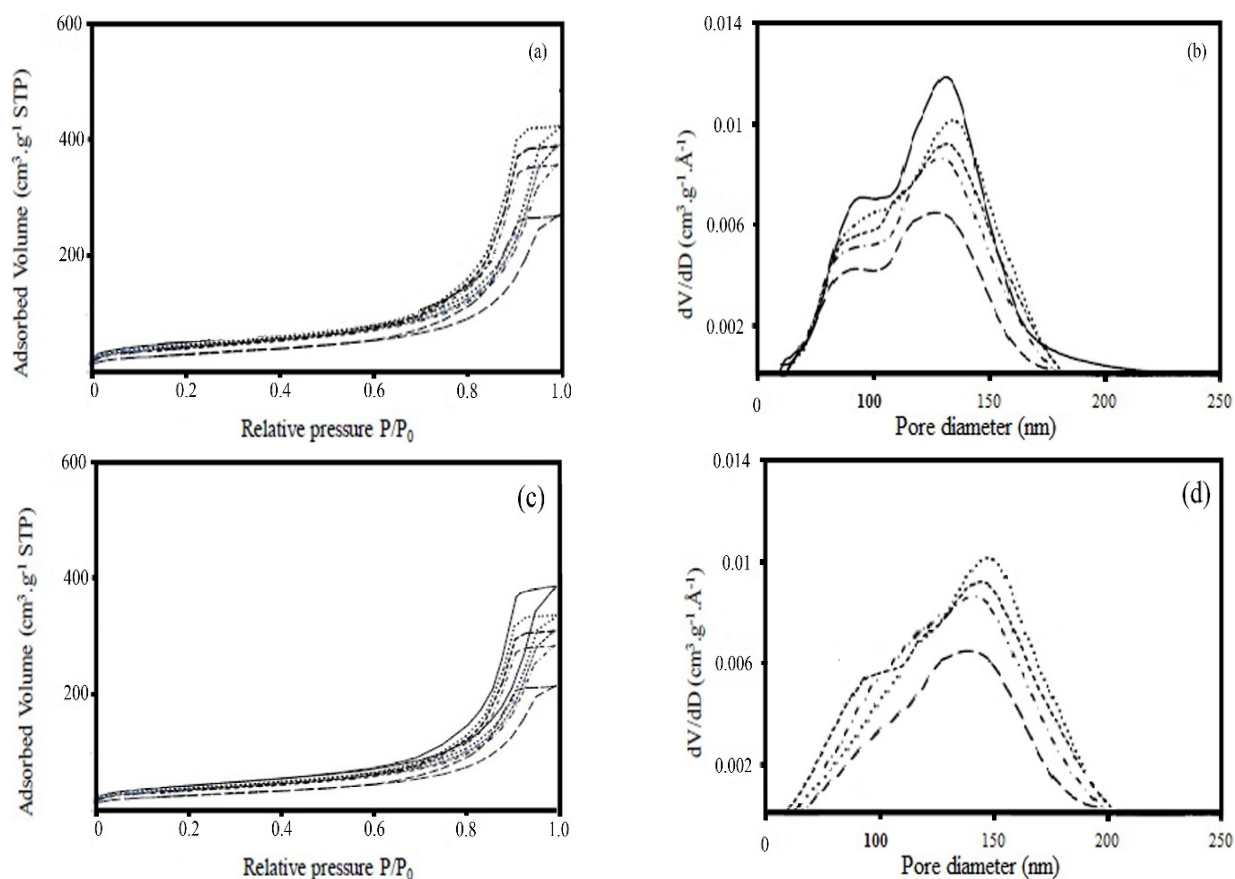


Fig. 5. Adsorption/desorption isotherms of N₂ for (a) before the test, (c) after the test, and pore size distribution curves for (a) before the test, (c) after the test.

The results indicated that as the temperature increases, CO conversion increases from 13.7% to 93.7%. Meanwhile, the rising temperature up to 310 °C causes a decrease in methanation then after passing this minimum apex, methane selectivity increases during the time-on stream tests. As a result, 300 °C can be considered to be the optimum operating temperature because of high total selectivity of produced C₅₊ and low CH₄; however, in this temperature, the conversion is just in a moderate amount. On the other hand, more increment in the reaction temperature leads to the formation of large amounts of coke as an unwanted by-product.

3.5. Gas hourly space velocity studies

A series of experiments was carried out to investigate the effect of the gas hourly space velocity (GHSV) on the activity and catalytic performance of the Co-Fe-Ni catalyst at the reaction conditions of H₂/CO=1, 300 °C, and the atmospheric precursor during variation of GHSV in the range of 3000-6000 h⁻¹.

The activity and hydrocarbon product distribution over the catalysts is shown in Fig. 8. From these data, it is clear that the activity of the catalysts is constant by

increasing GHSV from 3000 to 4800 h⁻¹. In addition, as it can be seen in Fig. 8, with the exception of 4800 h⁻¹, at this range of GHSV, no significant changes on C₁ and C₄₊ selectivity occurs.

Therefore, because of the higher total selectivity toward C₄₊, higher value of CO conversion and lower methane selectivity at the 4800 h⁻¹, this GHSV was chosen as the optimum gas space velocity.

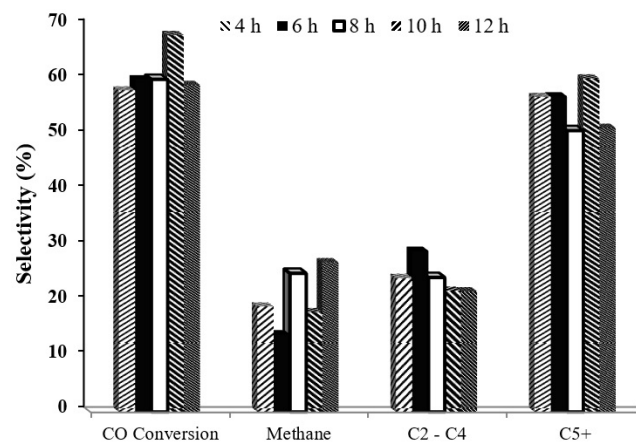


Fig. 6. Effect of calcination time on the catalytic performance of Co-Fe-Ni catalyst.

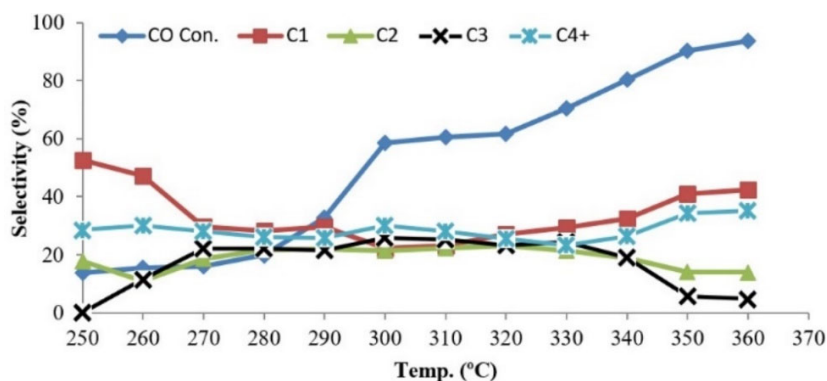


Fig. 7. Effects of reaction temperature on the catalytic performance of Co-Fe-Ni catalyst.

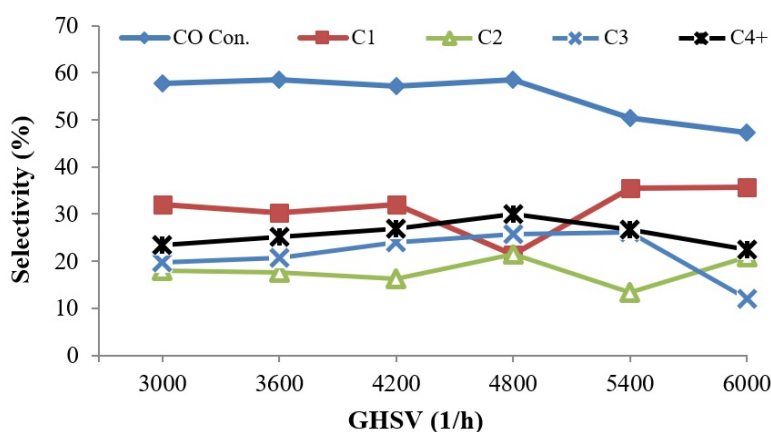


Fig. 8. Effect of gas hourly space velocity on the catalytic performance of Co-Fe-Ni catalyst.

3.6. Thermal analysis

Thermal behavior of catalyst precursor was characterized using the TGA/DSC technique and data are presented in Fig. 9. For the catalyst precursor, three major weight losses were observed. The first stage between 60 °C to 150 °C can be due to the water evaporation from open pores which physically trapped in the precipitate.

The second weight loss with onset temperatures at around 180-310 °C can be attributed to the decomposition of hydroxyl, or basic nitrates precursor, so that decomposition of these temperature regions produce water and nitrogen oxides simultaneously. The third stage of weight loss, which occurs at temperatures around 380-510 °C, can be due to the decomposition of hydroxyl, or basic carbonates precursor.

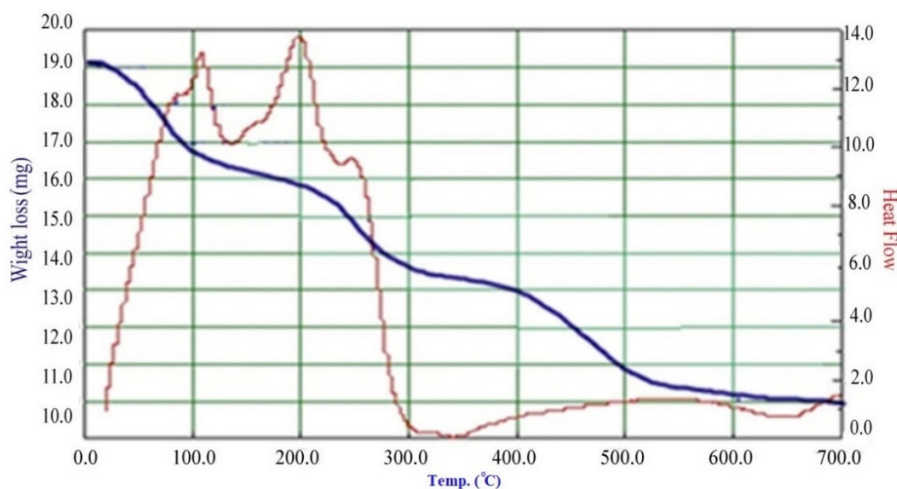


Fig. 9. DSC/TGA curves of the Co-Fe-Ni catalyst precursor.

This decomposition evolves water and carbon dioxide concurrently [29]. As it is shown in Fig. 9, DSC curve of the catalyst precursor is in agreement with the TGA results. Existence of three endothermic peaks in DSC curve provides further evidence for the presence of the various species and evaluates their thermal behavior.

4. Conclusions

The Co-Fe-Ni catalyst with the weight ratio 60:30:10 was prepared using the co-precipitation procedure and tested for CO hydrogenation in Fischer-Tropsch synthesis. The effects of some operating and calcination variables such as the temperature, gas hourly space velocity, time and agents on the catalytic performance and structure of the catalysts were investigated. The optimal calcination and operational conditions were found to be 550 °C for 6 h under air atmosphere and 260 °C with and GHSV=2200 h⁻¹ under atmospheric pressure. The optimal catalyst is found to be superior to the other catalysts in terms of higher CO conversion and better C₂-C₄ selectivity in FTS products. In addition, methane selectivity is suppressed from 27% to 14%. It was concluded that there was a direct relationship between calcinations temperatures and FT activity and reverse relationship with the formation of hydrocarbons. Calcination in nitrogen atmosphere also decreased the activity of the catalyst toward C₂-C₄ and C₅₊ selectivity. Also, different characterization techniques such as XRD, BET, TGA, DSC, and SEM show that the iron-cobalt-nickel catalysts are sensitive to the calcination and operation conditions. XRD patterns indicate the formation of iron carbides, Co and Ni metallic providing the FTS active sites. BET data show that increasing the calcination temperature up to 550 °C significantly enhances the surface area, pore volume and pore size distribution of the catalyst and with more increases in the temperature, all of these terms are reversed.

References

- [1] A.A. Muleja, Y. Yao, D. Glasser, D. Hildebrandt, *Ind. Eng. Chem. Res.* 56 (2017) 469-478.
- [2] T.O. Eschemann, K.P. de Jong, *ACS Catal.* 5 (2015) 3181-3188.
- [3] M. Zhuo, A. Borgna, M. Saeys, *J. Catal.* 297 (2013) 217-226.
- [4] K. Srirangan, L. Akawi, M. Moo-Young, C. Perry Chou, *Appl. Energy* 100 (2012) 172-186.
- [5] T. Taherzadeh Lari, A.A. Mirzaei, H. Atashi, *Catal. Lett.* 147 (2017) 1221-1234.
- [6] S. Golestan, A.A. Mirzaei, H. Atashi, *Int. J. Hydrogen Energy* 42 (2017) 9816-9830.
- [7] R. Liu, R. Liu, X. Ma, B. H. Davis, Z. Li, *Fuel* 211 (2018) 827-836.
- [8] H.J. Wan, B.S. Wu, T.Z. Li, Z.C. Tao, X. An, H.W. Xiang, Y.W. Li, *J. Fuel Chem. Technol.* 35 (2007) 589-594.
- [9] Z. Hajjar, M. Doroudian Rad, S. Soltanali, *Res. Chem. Intermed.* 43 (2017) 1341-1353.
- [10] M. Luo, W.D. Shafer, B.H. Davis, *Catal Lett.* 144 (2014) 1031-1041.
- [11] F. Pardo-Tarifa, S. Cabrera, M. Sanchez-Dominguez, M. Boutonnet, *Int. J. Hydrogen Energy* 42 (2017) 9754-9765.
- [12] J. Aluha, N. Abatzoglou, *J. Ind. Eng. Chem.* 50 (2018) 199-212.
- [13] X. Zhang, H. Su, Y. Zhang, X. Gu, *Fuel* 184 (2016) 162-168.
- [14] M. Dowlati, N. Siyavashi, H.R. Azizi, *Arab. J. Sci. Eng.* 43 (2018) 2441-2450.
- [15] I.R. Leith, M.G. Howden, *Appl. Catal.* 37 (1988) 75-92.
- [16] J.R. Anderson, M. Boudart, *Catalysis: Science and Technology*, Vol. 4, Springer-Verlag, Berlin, Heidelberg, 1983.
- [17] B.C. Enger, A. Holmen, *Catal. Rev. Sci. Eng.* 54 (2012) 437-488.
- [18] Z. Cheng-hua, Y. Yong, T. Zhi-chao, X. Hong-wei, L. Yong-wang, *J. Fuel Chem. Technol.* 34 (2006) 695-699.
- [19] G. Li, L. Hue, J.M. Hill, *Appl. Catal. A* 301 (2006) 16-24.
- [20] M. Ao, G.H. Pham, V. Sage, V. Pareek, *Fuel* 206 (2017) 390-400.
- [21] H.R. Azizi, A.A. Mirzaei, M. Kaykhahi, M. Mansouri, *J. Nat. Gas Sci. Eng.* 18 (2014) 484-491.
- [22] H.H. Storch, *Adv. Catal.* 1 (1948) 115-156.
- [23] H. Pichler, *Adv. Catal.* 4 (1952) 271-341.
- [24] F. Fischer, K. Mayer, *Brennst. Chem.* 12 (1931) 225-232.
- [25] D. Reinalda, J. Kars, *Eur. Pat. Appl. EP* 0421502 A2 (1991).
- [26] J. van de Loosdrecht, S. Barradas, E.A. Caricato, N.G. Ngwenya, P.S. Nkwanyana, M.A.S. Rawat, B.H. Sigwebela, P.J. van Berge, J.L. Visagie, *Top. Catal.* 26 (2003). 121-127.
- [27] M. Arsalanfar, A.A. Mirzaei, H.R. Bozorgzadeh, *J. Ind. Eng. Chem.* 19 (2013) 478-487.
- [28] A.A. Mirzaei, S. Shahryari, M. Arsalanfar, *J. Nat. Gas Sci. Eng.* 3 (2011) 537-546.
- [29] Z. Tao, Y. Yang, M. Ding, T. Li, H. Xiang, Y. Li, *Catal. Lett.* 117 (2007) 130-135.
- [30] M. Ding, Y. Yang, Y. Li, T. Wang, L. Ma, C. Wu, *Appl. Energy* 112 (2013) 1241-1246.
- [31] G. Ertl, H. Knözinger, J. Weitkamp, *Handbook of Heterogeneous Catalysis Vol. 1*, Wiley-VCH, Weinheim, 1997.
- [32] S.H. Song, S.B. Lee, J.W. Bae, P.S. Sai Prasad, K.W. Jun, Y.G. Shul, *Catal. Lett.* 129 (2009) 233-239.
- [33] T. Herranz, S. Rojas, F.J. Pérez-Alonso, M. Ojeda, P. Terreros, J.L.G. Fierro, *Appl. Catal. A* 311 (2006) 66-75.
- [34] N. Lohitharn, J.G. Goodwin Jr., *J. Catal.* 260 (2008) 7-16.
- [35] A.A. Mirzaei, R. Sarani, H.R. Azizi, S. Vahid, H.O. Torshizi, *Fuel.* 140 (2015) 701-710.
- [36] M. Feyzi, M. Irandoust, A.A. Mirzaei, *Fuel Process. Technol.* 92 (2011) 1136-1143.